scientific reports

Check for updates

OPEN

Lipidomic study of kidney in a mouse model with urine flow obstruction

Divyavani Gowda[1,8], Md. Abdul Masum[2,3,8]✉, Siddabasave Gowda B. Gowda[1,4], Chandra Shekhar[1,5], Md. Zahir Uddin Rubel[3], Shunnosuke Kira[3], Osamu Ichii[3,6], Yasuhiro Kon[3], Hitoshi Chiba[7] & Shu-Ping Hui[1]✉

Obstructed urine flow is known to cause structural and functional kidney damage leading to renal fibrosis. However, limited information is available on the change in kidney lipids during urinary tract obstruction. In this study, we investigated the change in lipidome in a mouse model with unilateral ureteral obstruction (UUO). The establishment of the UUO model was confirmed by histopathological examination using transmission electron microscopy. Untargeted liquid chromatography/mass spectrometry was carried out over a time course of 4 and 7 days. Compared to the sham control, the UUO kidney at 7 days showed dilatation of the renal tubule with loss of brush borders and thickening of the capillary endothelium. In the kidney lipidomes obtained from the UUO 7 days group compared to the control, a significant decrease of ceramide, sphingomyelin, phosphatidylcholine, lysophospholipids, and phosphatidylethanolamine was observed, whereas cholesteryl esters, free fatty acids, phosphatidylglycerol, and cardiolipins were significantly increased. The present study revealed the disturbed lipid metabolism in the UUO model, which may provide a clue to potential lipid pathways and therapeutic targets for the early stage of renal fibrosis.

Keywords Lipid, Liquid chromatography, Mass spectrometry, Kidney injury, Unilateral ureteral obstruction, Renal tubulointerstitial lesion

Lipids consist of the most abundant metabolites in circulation and serve as an integral part of cell structure and function[1]. Lipidomics refers to the global study of lipid species and their biological functions within biological systems[2]. Their alterations are linked with disease severity and outcome[3], therefore, an abundance of individual lipid molecular species in plasma may be indicative of the variety of specific human diseases[4]. The utility of large-scale lipidomic profiling has been shown in several systemic disorders[1]. Recent, promising data indicate lipid profiling is a powerful discovery tool in nephrology research[5,6]. Obstructive nephropathy, also known as uropathy is a common clinical case[7] it's serious and irreversible consequences as it can lead to renal failure and interfere with the maturation of the kidneys. Additionally, it may also result in acute kidney injury (AKI) or chronic kidney disease (CKD)[8].

Ureteral obstruction is known as one of the prevalent clinical renal disorders that can occur at any age[9]. Studies have demonstrated that prolonged ureteral obstruction can lead to nephropathy and chronic kidney injury[10]. Early detection enables effective treatment and reversal[9]. One commonly used model for studying obstructive nephropathy is a unilateral ureteral obstruction (UUO). In this experimental procedure, the left ureter is typically ligated using a silk thread[11]. UUO occurs in approximately 1 in 1000 adults[12]. This condition causes an increase in hydrostatic pressure due to urine stagnation. Which then triggers the renin-angiotensin system (RAS) via the production of angiotensin II (Ang II)[13]. Ang II activates nicotinamide adenine dinucleotide phosphate

[1]Faculty of Health Sciences, Hokkaido University, Kita-12 Nishi-5, Kita-ku, Sapporo 060-0812, Japan. [2]Department of Anatomy, Histology and Physiology, Faculty of Animal Science and Veterinary Medicine, Sher-e-Bangla Agricultural University, Dhaka 1207, Bangladesh. [3]Laboratory of Anatomy, Department of Basic Veterinary Medicine, Faculty of Veterinary Medicine, Hokkaido University, Sapporo 060-0818, Japan. [4]Graduate School of Global Food Resources, Hokkaido University, Kita 9, Nishi 9, Kita-ku, Sapporo 060-0809, Japan. [5]Departments of Physiology, Medicine, Molecular Biology Immunology and Biochemistry, and Pharmaceutical Sciences, University of Tennessee Health Science Center, Memphis, TN 38163, USA. [6]Laboratory of Agrobiomedical Science, Faculty of Agriculture, Hokkaido University, Sapporo 060-0809, Japan. [7]Department of Nutrition, Sapporo University of Health Sciences, Nakanuma, Nishi-4-3-1-15, Higashi-ku, Sapporo 007-0894, Japan. [8]These authors contributed equally: Divyavani Gowda and Md. Abdul Masum. ✉email: masum@sau.edu.bd; keino@hs.hokudai.ac.jp

(NADPH) oxidases (NOXs), resulting in the production of reactive oxygen species (ROS). These ROS lead to oxidative stress, inflammation, and cell death through apoptosis or necrosis[11,14]. Such mechanisms also activate myofibroblasts from resident fibroblasts, which then replace lost epithelial cells with extracellular matrix (ECM) and promote progressive fibrosis[14–16].

Previous studies have shown that kidneys affected by UUO display more noticeable metabolic changes over time compared to those in the sham control groups[16]. Dysregulated lipid metabolism leading to dyslipidemia is an often under-recognized, but nearly universal, complication of persistent nephrotic syndrome[17,18]. In the last decade, many wide-ranging research studies have been performed to find new biomarkers to detect early impaired kidney function[18]. Such advances also provide opportunities to expand diagnostic capabilities through biomarker discovery efforts, identify novel alterations in involved pathways, and potentially identify targets amenable to the intervention[3]. Rovin et al. demonstrated that the UU-obstructed rat kidney releases a chemotactic factor that behaves as a lipid, which may account for the mononuclear cell infiltrate observed during obstruction[19].

To evaluate whether lipidome from renal tissues could provide information, a test was carried out on the UUO. It is believed that experimental UUO in rodents mimics chronic obstructive nephropathy in humans but at an accelerated rate[11]. Our investigation aimed to determine the lipid alterations in renal tissues following obstruction and assess their potential as predictive markers. This well-characterized model system allowed us to assess lipidomic changes over a time course.

Materials and methods

Materials

The solvents/eluent for lipid extraction and analysis such as chloroform, 1 M aqueous ammonium acetate, methanol, and isopropanol of LC/MS grade were purchased from Wako Pure Chemical Industries, Ltd. (Osaka, Japan)., EquiSPLASH Lipidomix quantitative standard for mass spectrometry (catalog No. 330731, consists of phosphatidylethanolamine (PE) (15:0–18:1(d7)), phosphatidylcholine (PC) (15:0–18:1(d7)), phosphatidylglycerol (PG) (15:0–18:1(d7)), phosphatidylserine (PS) (15:0–18:1(d7)), phosphatidylinositol (PI) (15:0–18:1(d7)), lysophosphatidylethanolamine (LPE) (18:1(d7)), lysophosphatidylcholine (LPC) (18:1(d7)), ceramide (Cer) (d18:1/15:0 (d7)), sphingomyelin (SM) (d18:1/18:0(d9)), monoacylglycerol (18:1(d7)), diacylglycerol (DAG) (15:0–18:1(d7)), triacylglycerol (TAG) (15:0–18:1(d7)–15:0), and cholesteryl ester (CE) (18:1(d7)) and oleic acid-d9 the internal standards for lipid quantification were obtained from Avanti Polar Lipids (Alabaster, AL, USA).

Animal and UUO treatment

UUO models are one of the popular experimental models of the renal tubulointerstitial lesion (TIL) or injury. In this study, to create the TIL using the UUO model, 8-weeks-old male C57BL/6 mice ($N=12$) were subjected to UUO for 7 days. Briefly, mice were deeply anesthetized with a mixture of 0.3 mg/kg medetomidine (Kyoritsu Seiyaku, Japan), 4 mg/kg midazolam (Astellas Pharma, Japan), and 5 mg/kg butorphanol (Meiji Seika Pharma, Japan), and laparotomy in the sublumbar region was performed to ligate the right ureter tightly with silk thread at the renal hilus. Buprenorphine hydrochloride (Otsuka Pharmaceuticals, Japan) was injected intraperitoneally at a dose rate of 0.3 mg/kg as an analgesic. Recovery from anesthesia was facilitated by intraperitoneal administration of 0.3 mg/kg atipamezole (Zenoaq, Japan). For mRNA analysis, a second set of UUO experiments were conducted in 8-weeks-old male C57BL/6 mice ($N=8$).

Histopathological examination

Small pieces of kidney tissues were fixed with neutral buffer formalin and 4% paraformaldehyde in 0.1 M phosphate buffer, or 2.5% glutaraldehyde in 0.1 M phosphate buffer. Kidney sections were cut at a thickness of 3 µm and stained with the periodic acid Schiff-hematoxylin (PAS-H) to determine the histopathological condition. Immunostaining for B220, CD3, and Iba1 was performed to detect B-cells, T-cells, and macrophages, respectively as described in our previous study[20,21]. Transmission electron microscopy analysis was conducted on the same conditions as described in our earlier studies[21].

Extraction and analysis of lipids

Lipids were extracted from the kidney tissue by the biphasic Folch method[6], with slight modifications established earlier in our lab[22,23]. In brief, 16–82 mg of whole kidney tissues were weighed into a 2 mL Eppendorf tube and 5–6 ceramic beads of diameter 1.4 mm were added (catalog no. 15-340-159, Fisherbrand). Homogenized the mixture using a Bead Mill 4 (Fisherbrand) for two cycles of 30 s each. Then, 10 volumes of ice-cold methanol were added, and homogenization was repeated for another 30 s. Exactly, 100 µL of the methanolic homogenate were transferred to an Eppendorf tube, to this, 100 µL of the internal standard mixture in methanol was added (final concentration of 10 µg/mL EquiSPLASH Lipidomix and 100 µg/mL of oleic acid-d9) and the mixture was vortexed at 3500 rpm for 30 s. Subsequently, 400 µL of chloroform was added and vortexed for 5 min, and 100 µL of milli-Q was added with an additional vortex for 30 s. The extracts were centrifuged (at 15,000 rpm for 10 min at 4 °C) and the lower organic layer was transferred to a vial, while the upper layer was re-extracted with an additional 400 µL of chloroform. The combined organic extracts were concentrated under a vacuum and redissolved in 100 µL of methanol with gentle vortexing and centrifuged (at 15,000 rpm for 10 min at 4 °C). The centrifugate was then transferred to a 0.3 mL SC-vial (catalog. No. 1030-14,110, GL Sciences, Tokyo, Japan) and 10 µL of each sample was injected into the LC/MS.

A prominence UFLC system (Shimadzu Corp., Kyoto, Japan) coupled with an LTQ Orbitrap MS (ThermoFisher Scientific Inc., San Jose, CA) was used for the lipid analysis. The separation of lipids was achieved using an Atlantis T3 C18 column (2.1 × 150 mm, 3 µm, Waters, Milford, MA), maintained at 40 °C with a total flow rate of 0.2 mL/min from three mobile phases (A: 10 mM CH_3COONH_4, B: isopropanol, and C: methanol). The linear

gradient and mass spectrometric conditions for positive (*m/z* 160–1900) or negative (*m/z* 100–1750) ionization are identical to our previous report[22,23]. Briefly, the gradient in negative mode analysis was set as 0–1 min (30% B and 35% C), 1–14 min (80% B and 10% C), and 14–27 min (85% B and 10% C). Whereas, in positive mode analysis the gradient was set as follows: 6% B and 90% C (0–1 min), 83% B and 15% C (1–10 min), 83% B and 15% C (10–19 min), 6% B and 90% C (19–19.5 min), In both ionization modes the column re-equilibration was done for 3 min. The raw data were processed using MS DIAL (version 4.2) software (RIKEN, Wako, Japan) for the alignment and identification of lipid species based on MS/MS spectral matching. The concentration (in pmol) of the lipid molecular species was calculated by taking the peak intensity ratios of the analyte to the internal standard and normalized by the weight of the kidney tissue used. The details about the lipid quantification including peak area of lipid metabolites without normalization, weight of kidney used for analysis, and concentration of spiked internal standards were provided in the supporting information. The list of identified lipid metabolites and their concentrations are provided in the supporting information Table S1.

RNA extraction and quantitative PCR

Total RNA was extracted from the obstructed kidney (whole kidney) using TRIzol reagent (Thermo Fisher Scientific). Purified total RNA was used as a template to synthesize cDNA using the ReverTra Ace quantitative polymerase chain reaction (qPCR) RT Master Mix with gDNA Remover (Toyobo, Osaka, Japan). qPCR analysis was performed using THUNDERBIRD SYBR qPCR Mix (Toyobo) and gene-specific primers. The specific forward and reverse primers used for qPCR are listed in supporting information in Table S2.

Statistical analysis

Data were plotted using Excel 2016 or Prism 8.1 (GraphPad Software, San Diego, CA, USA). Two-way or one-way ANOVA analysis with a correction for multiple comparisons if necessary and considered significant when $p < 0.05$. Data are the mean ± SEM. Data visualizations were performed using Metabo Analyst 5.0.

Ethical statement

All the animal experiments were conducted in accordance with ARRIVE guidelines (https://arriveguidelines.org) with prior approval from the Institutional Animal Care and Use Committee of the Faculty of Veterinary Medicine, Hokkaido University (approval No. 16-0124). The authors adhered to the approved Guide for the Care and Use of Laboratory Animals of Hokkaido University, Faculty of Veterinary Medicine (approved by the Association for Assessment and Accreditation of Laboratory Animal Care International).

Results

Tubulointerstitial lesions (TIL) development in Unilateral Ureteral Obstruction (UUO) kidney

Mice were subjected to UUO for different periods and successfully developed TIL in a time-dependent manner (Fig. 1). Sham control mice did not show any TIL but UUO kidney at 4 days showed mild dilatation of tubules whereas, severe TILs were found in UUO kidney at 7 days (Fig. 1a). Similarly, more infiltrating B-cells, T-cells, and macrophages were found in UUO kidney at 7 days compared to UUO kidney at 4 days and sham control kidney (Fig. 1b–d). As severe TIL was found in the UUO kidney at 7 days, we clarified it by transmission electron microscopy analysis. Sham control kidney showed normal tubular epithelium containing few regular empty spaces, and peritubular capillary (Fig. 2a) but the UUO kidney at 7 days showed dilatation of renal tubules with loss of brush border, thickening, and loss of capillary endothelial fenestration, many regular empty spaces in tubular epithelium indicating more lipid accumulation in injured tubule (Fig. 2b). Moreover, thickening of the capillary endothelium and loss of its fenestration was also found in UUO kidney. The changes in lipid pathway-related genes are measured by quantitative PCR and the results are shown in Fig. 2c. The lipid binding protein Apolipoprotein E (ApoE), lipid droplet promoting genes Perilipin (Plin1 and Plin2), and fatty acid metabolism associated gene acyl-CoA synthetase long-chain family member 4 (Acsl4) are upregulated in UUO kidney at 7 days compared to control kidney. The phospholipid metabolism-related gene lysophosphatidylcholine acyltransferase 3 (Lpcat3) is decreased in the UUO kidney at 7 days whereas Phosphatidylserine decarboxylase (Pisd) was unchanged. Further, the sphingolipid metabolism associated genes Serine palmitoyltransferase long chain base subunit 1 (Sptlc1) was also unchanged but Sphingomyelin phosphodiesterase (Smpd1) is significantly decreased in UUO kidney at day 7 compared to control. The altered lipid pathways-related genes indicate the disturbed lipid metabolism in the UUO kidney.

Change in sphingolipids and sterols levels in the progression of UUO kidney

The amounts of sphingolipids such as ceramides, hexosylceramides, sphingomyelin, and sterols mainly cholesteryl esters characterized in the kidney samples are shown in Fig. 3. Among all major lipid subclasses, sphingomyelin levels are predominant followed by cholesteryl esters and ceramides. When compared with control, sphingomyelins, and ceramides were found to decrease, whereas cholesteryl esters were observed to increase in UUO kidneys. Ceramide levels are started to decrease from day 4 and further reduced on day 7 of the UUO kidney. The ceramide molecular species (Fig. 3a) that were abundant and significantly decreased are Cer (d18:1/24:0) and Cer (d18:1/24:1) respectively. Hexosylceramides (Fig. 3a) such as HexCer (d18:1/24:0; O), and HexCer (d18:1/24:1) are reduced on day 4 of UUO. The sphingomyelin (Fig. 3b) levels also showed the same trend as ceramides i.e. decreased on the 4th day and further decreased on the 7th day of UUO. The molecular species which are significantly decreased are SM (d18:1/16:0), SM (d18:1/16:1), SM (d18:1/22:0), SM (d18:1/24:1) and SM (d18:1/23:0) respectively. The SM (d18:1/24:1) is the most abundant molecular species among sphingomyelins. The levels of sterols mainly cholesteryl esters characterized in the study are depicted in Fig. 3c. Results show a significant increase of CE (18:2), and total CE (sum of individual molecular species) in the UUO group compared to control.

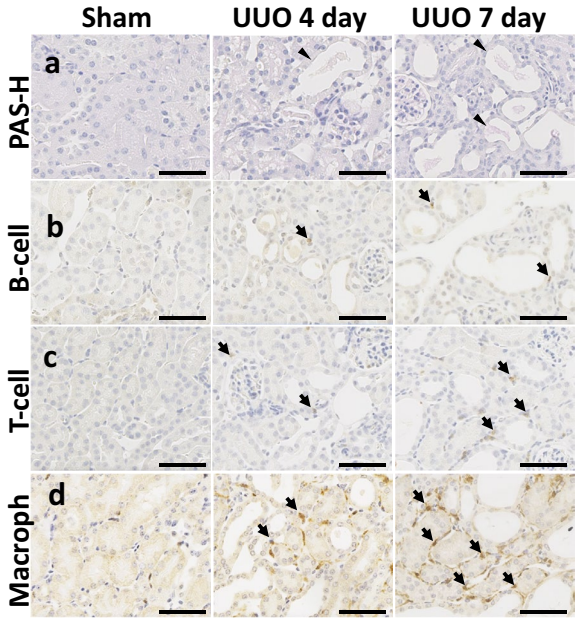

Figure 1. Tubulointerstitial lesion (TIL) in unilateral ureteral obstruction (UUO) mouse models. (**a**) Histopathological features of TILs in sham control and UUO mice. The tubular injury in the UUO kidney is characterized by the dilatation of tubules with the urinary cast (arrowhead). Mild and severe TIL were observed in UUO kidney at 4 and 7 days respectively. Periodic acid Schiff-hematoxylin (PAS-H) staining. (**b**–**d**) Analysis of $B220^+$ B-cell, $CD3^+$ T-cells, and Iba-1^+ macrophage (arrows) infiltration in sham control and TILs of UUO mice. Immunohistochemistry. All bars = 100 µm.

Change in fatty acyls glycerophospholipids and glycerolipids levels in the progression of UUO kidney

The analysis results of the amounts of fatty acyls such as free fatty acids (FAs), glycerophospholipids including lysophospholipids (lysophosphatidylcholine (LPC), lysophosphatidylethanolamine (LPE), lysophospahtidylinositol (LPI), and lysophosphatidylglycerol (LPG)) and phospholipids (phosphatidylinositol (PI), and phosphatidylserine (PS)) characterized in the kidney samples are shown in Fig. 4. FAs level are almost unchanged between control and at day 4 of UUO but increased slightly at day 7 of UUO. The FAs such as F18:1, FA18:2, FA 20:4, and FA 22:5 have shown an increasing trend at day 7 of UUO compared to controls. In contrast, the lysophospholipids such as LPE 16:0, LPE 18:0, LPE 18:1, and LPC 18:0 are significantly reduced at day 7 of UUO. The PIs such as PI (18:0/20:3), and PI (18:0/20:4) are decreased at day 7 of UUO compared to controls whereas, PS (18:0/18:1) and PS (22:0/18:1) appear to be significantly increased at day 4 and day 7 of UUO.

The amounts of phospholipids including phosphatidylcholine (PC), phosphatidylethanolamine (PE), phosphatidylglycerol (PG), and cardiolipins (CL) characterized in the kidney samples of UUO mice model are shown in Fig. 5. Generally, the PCs levels are shown to be decreasing from control to day 7 of UUO. The molecular species such as PC (16:0/18:1), PC (18:0/18:1), PC (18:0/18:2), PC (18:0/20:4), and PC (16:0/22:6) are significantly decreased at 4 and 7 days of UUO compared to controls. PEs also showed to have a similar trend as PCs with a sharp decrease from control to day 7 of UUO. In particular, PEs having linoleic acid acyl chain linoleic acid (PE (18:0/18:2), PE (18:1/18:2)), arachidonic acid acyl chain (PE (16:0/20:4), PE (18:0/20:4), PE (O-16:1/20:4), and docosahexaenoic acid acyl chain (PE (16:0/22:6), PE (18:0/22:6), PE (18:1/22:6), PE (O-18:1/22:6), PE (O-18:2/22:6)) are significantly reduced at 4 and 7 days of UUO compared to controls. In contrast, PGs showed mixed variations for example PG (16:0/18:1), and PG (16:0/20:2) decreased at day 7 of UUO whereas PG (22:6/22:6) increased at 4 and 7 days of the UUO group compared to controls.

Finally, the relative amounts of glycerolipids mainly triacylglycerols (TAG) characterized in kidney samples of the UUO model are depicted in Fig. 6. TAGs showed a general trend that as a slight decrease in their levels at day 4 of UUO but a sharp increase at day 7 of UUO compared to controls. The significantly increased TAGs are TAG 52:2, TAG 52:4, TAG 54:2, TAG 54:3, TAG 54:7, TAG 56:3, and TAG 56:4 at day 7 of UUO compared to controls.

Discussion

In this study, we showed that UUO successfully developed TIL in a time-dependent manner as we described previously[20,21]. Therefore, the UUO model was used in this study to determine lipidomic changes that were observed in renal tissues after obstruction and to identify lipidomic changes. Sphingolipids play an important role in maintaining proper renal functions, since by affecting podocyte functioning, they can alter the leakages into the urine[24]. Several studies report sphingolipid rheostat to play a major role in kidney diseases based on the evidence showing podocyte damage caused by an increase in ceramide levels through mitochondrial dysfunction that leads to renal failure[25–28].

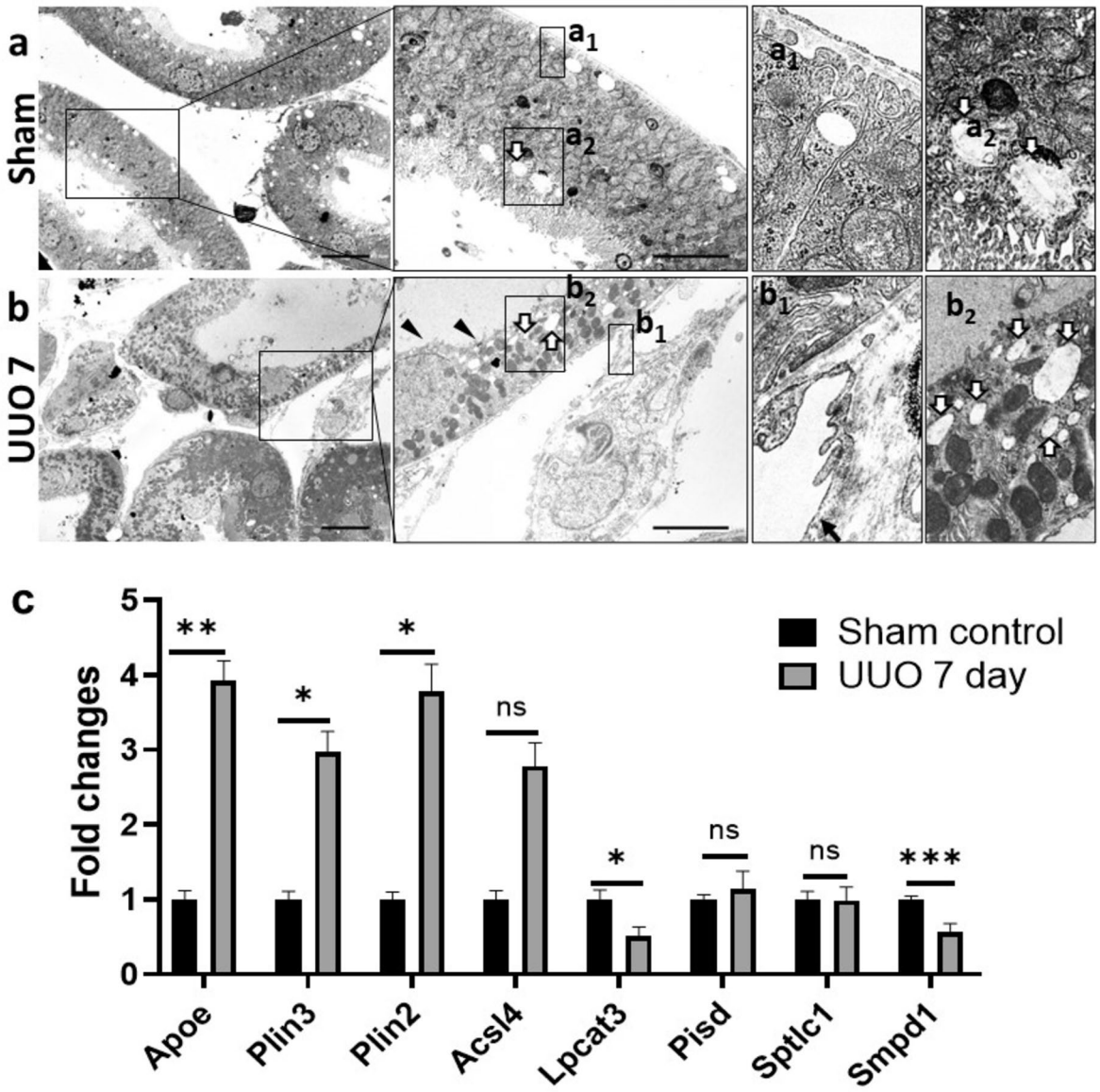

Figure 2. Ultrastructural changes of tubule interstitium and changes in lipid pathway-related genes in UUO mouse model at 7 days. (**a**). Sham control kidney shows normal tubules. Peritubular capillary shows normal thickening and fenestration of endothelium ($\mathbf{a_1}$). Few regular empty spaces (thick arrow) are present in the tubular epithelium ($\mathbf{a_2}$) (**b**). UUO kidney at 7 days shows dilatation of tubule with loss brush border (arrowheads). Thickening and loss of fenestration of capillary endothelium (arrow) are also observed in UUO kidney ($\mathbf{b_1}$). Many regular empty spaces (thick arrows) are present in the tubular epithelium of the UUO kidney ($\mathbf{b_2}$). (**c**) Changes in expression levels of lipid pathway-related genes between sham control (n = 4) and UUO kidney (n = 4) at 7 days (Student *t*-test, one-tailed, $^{**}p < 0.01$, $^{*}p < 0.05$, *ns*: non-significant).

Reports of previous studies have demonstrated that ceramides, sphingomyelin, and cholesteryl esters are significantly associated with kidney disorders such as UUO[29–31]. KEGG orthology analysis by Chen et al. identified 48 significantly altered pathways, which include sphingolipid metabolism, in the UUO rats[29]. Prolonged UUO (at least 14 days duration) increases renal ceramide in neonatal rats[30]. Long-chain ceramides were found significantly downregulated in both the fibrotic human kidney cortex and fibrotic murine kidney compared to control samples[32]. UUO of 24 h duration results in a 20% decrease in cholesterol and cholesteryl esters and a 12% fall in sphingomyelin content of tubular cells of the kidney of dogs[31]. Our study showed a decrease in the levels of both sphingomyelin and ceramide on both 4 and 7 days of UUO compared to the control (Fig. 3). Although the enzyme associated with the first step of sphingolipid biosynthesis, sptlc1 is unchanged between control and UUO groups, Smpd1 an enzyme hydrolyses the sphingomyelin to ceramide is decreased in UUO kidney at day 7 (Fig. 2c), which possibly explains the cause for lower ceramide levels in UUO kidney. Since both of these lipids cause altered renal functioning[24] and podocyte damage through mitochondrial dysfunction[25–28], the UUO model did not seem to be significantly regulated by sphingomyelin and ceramide. However, a decrease in cholesteryl esters has been previously reported in the UUO model of dogs where changes in solute transport and altered

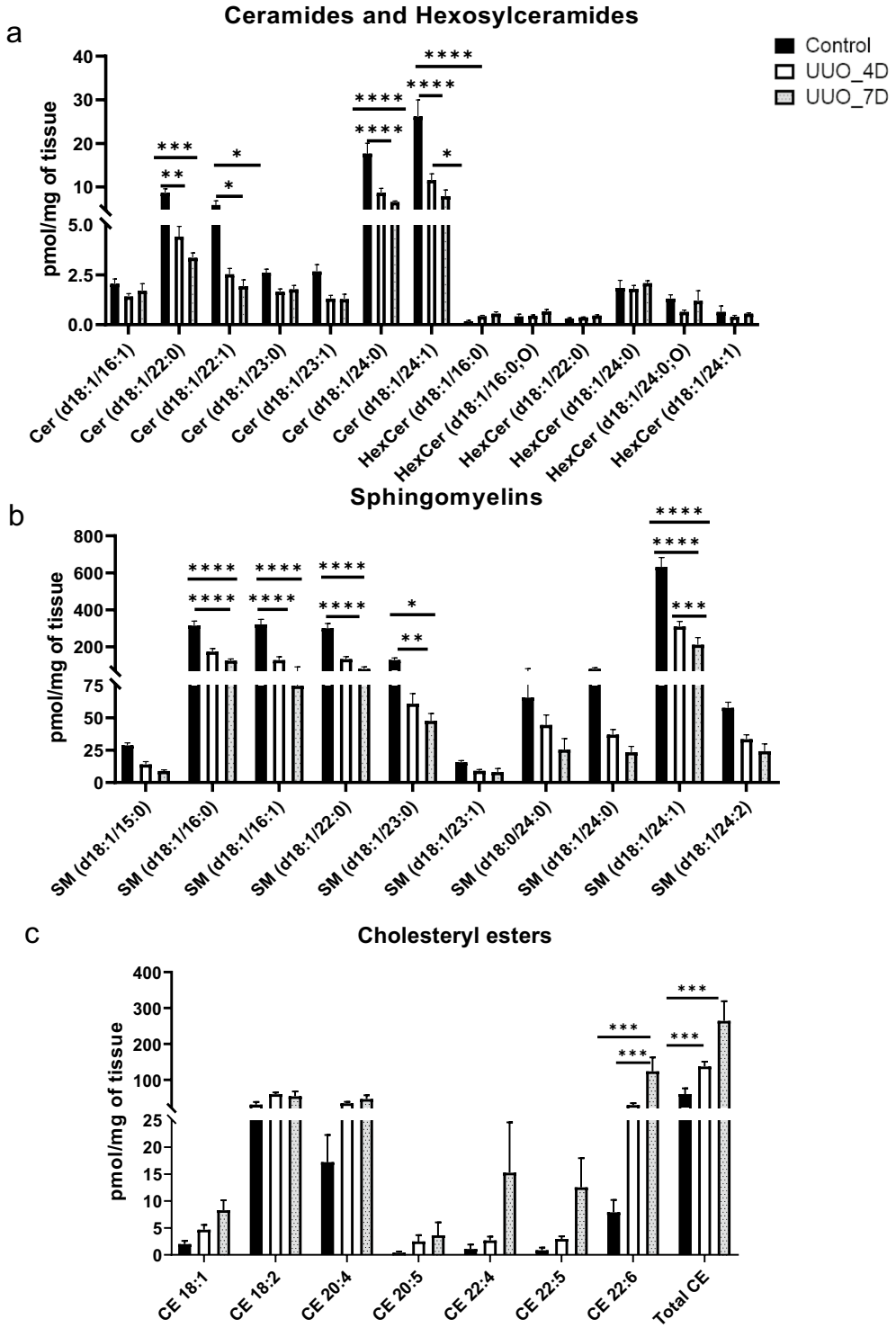

Figure 3. The concentrations of sphingolipids and sterols were determined in kidney samples. (**a**). Amount of ceramides and hexosylceramides, (**b**) sphingomyelin, and (**c**) cholesteryl esters measured in kidney samples collected from control and UUO model mice. One-way ANOVA Tukey's multiple comparison tests were applied. A value of $p < 0.05$ (95% confidence level) is considered statistically significant, $^{*}p < 0.05$, $^{**}p < 0.01$, $^{***}p < 0.001$, and $^{****}p < 0.0001$.

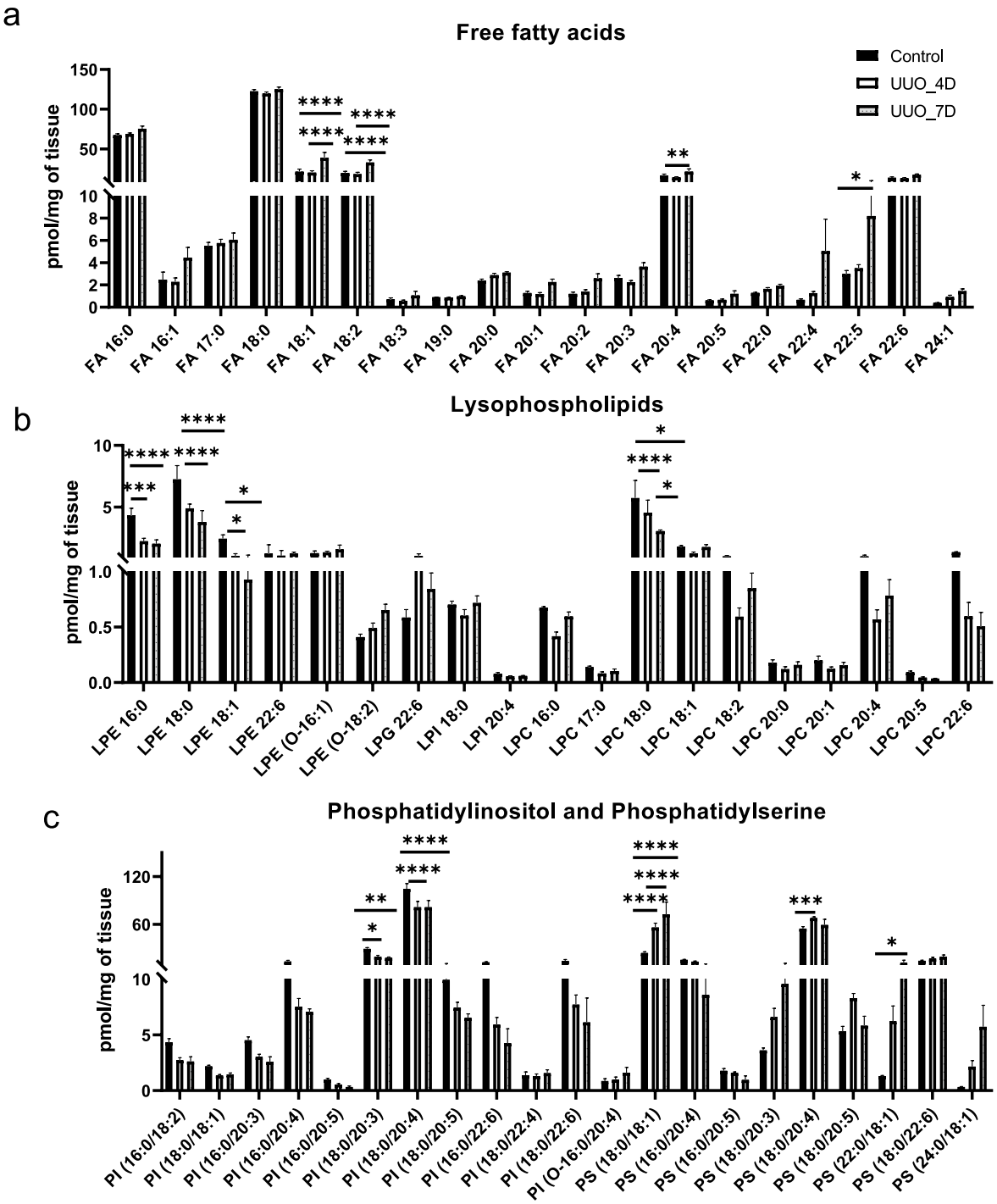

Figure 4. The concentrations of fatty acyls and glycerophospholipids (PS, PI) were determined in the kidney samples. (**a**) Free fatty acids (**b**) lysophospholipids, (**c**) Phosphatidylinositol (PI), and Phosphatidylserine (PS). One-way ANOVA Tukey's multiple comparison tests were applied. A value of $p < 0.05$ (95% confidence level) is considered statistically significant, $^{*}p < 0.05$, $^{**}p < 0.01$, $^{***}p < 0.001$, and $^{****}p < 0.0001$.

response to hormones were postulated as a reason[31]. Since a change in the stoichiometry of sphingomyelin and cholesteryl ester is accompanied by alterations in the cholesteryl ester homeostasis[33,34], therefore a collective regulation might be drawn from the UUO model of rats.

Fatty acid accumulation in proximal tubules plays a fundamental role in the progress of kidney disease[35]. Dysregulated lipid metabolism with disturbed FA metabolism may induce renal damage and chronic renal failure (CRF)[36,37]. Interestingly, forced overexpression of liver-type fatty-acid-binding protein in the kidney of mice was found to protect against renal inflammation and damage due to UUO[38]. When investigating the dynamic profile of metabolites and lipids in UUO using mass spectrometry, Banerjee et al. detected species of lipids including FAs that become more prominent over the time course in kidneys subject to UUO than sham controls[16]. In our

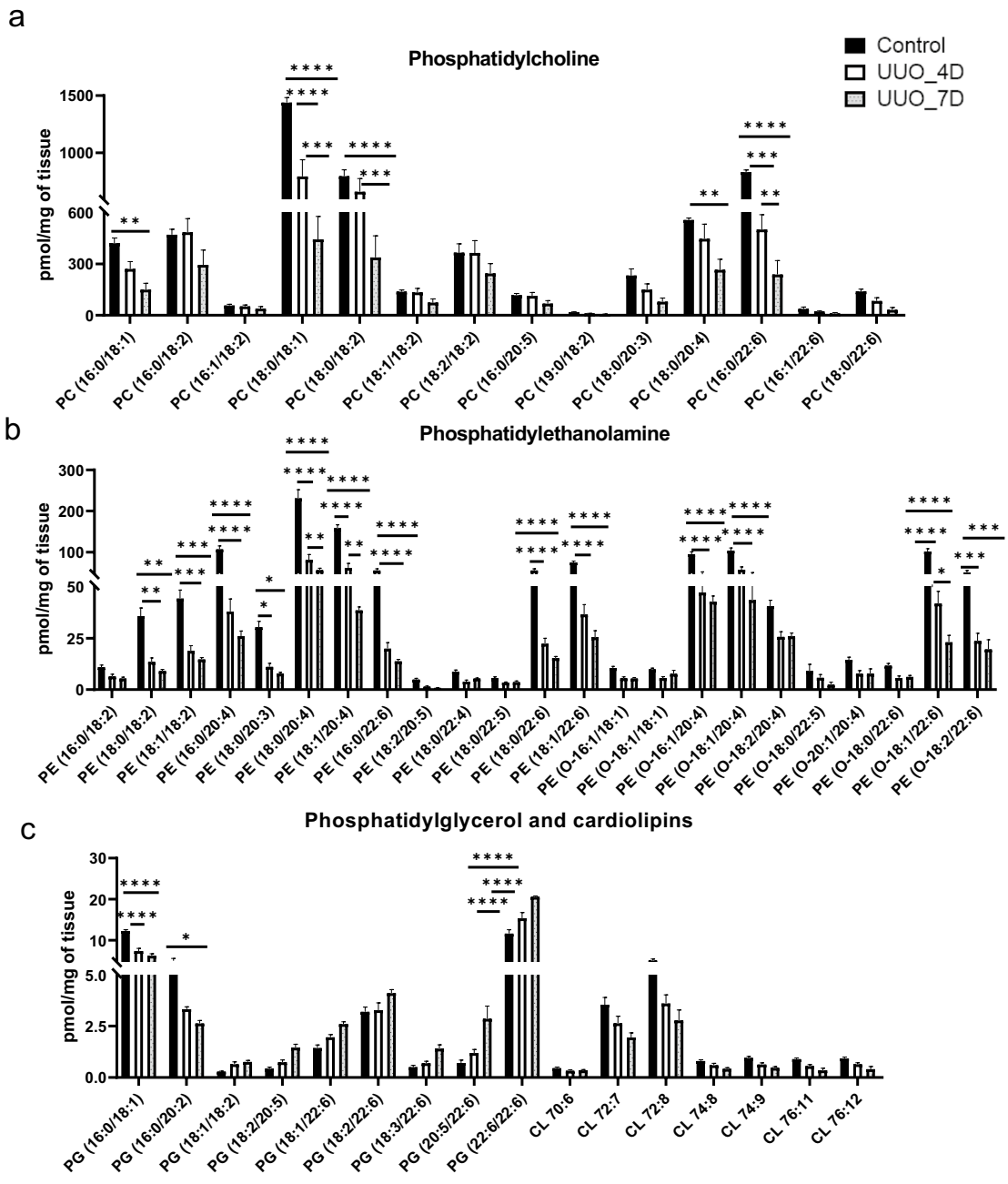

Figure 5. The concentrations of glycerophospholipids (PC, PE, PG, CL) were determined in kidney samples (**a**) Phosphatidylcholine (PC), (**b**) phosphatidylethanolamine (PE), (**c**) Phosphatidylglycerol (PG), and cardiolipins (CL). One-way ANOVA Tukey's multiple comparison tests were applied. A value of $p < 0.05$ (95% confidence level) is considered statistically significant, $^{*}p < 0.05$, $^{**}p < 0.01$, $^{***}p < 0.001$, and $^{****}p < 0.0001$.

study, FAs data showed no drastic changes but a slight increment on both 4 and 7 days of UUO compared to the control (Fig. 4). In favour of these results, the long-chain fatty acid metabolism enzyme Acsl4 is shown to be upregulated in UUO kidney at day 7 compared to control. A previous study demonstrated that inhibition of Acsl4 could protect fibrotic kidney disease via ameliorating tubular ferroptosis cell death[39]. Since excess FAs may lead to podocyte structural damage that results in glomerulopathy and CRF[37], FAs seem not to be crucial in UUO pathogenicity.

Lysophospholipids are involved in the pathogenesis of renal fibrosis[40]. Lysophosphatidic acid (LPA) (a lysophospholipid mediator) is reported to be about threefold higher in patients with renal failure compared to controls. Another study found that UUO treatment resulted in no significant increases in LPA production in rats, which might indicate its limited role in renal functions after UUO, but not circulatory propagation of renal injury[41]. Despite LPA was not measured in this study due to technical limitations, our results demonstrate decreased lysophospholipids on both 4 and 7 days of UUO (Fig. 4). The decrease in lysophospholipids could be explained by the significantly decreased expression of Lpcat3 levels in UUO kidney at day 7. For physiological processes such as cell polarization, filtration, solute reabsorption, and signal transduction, the kidney depends

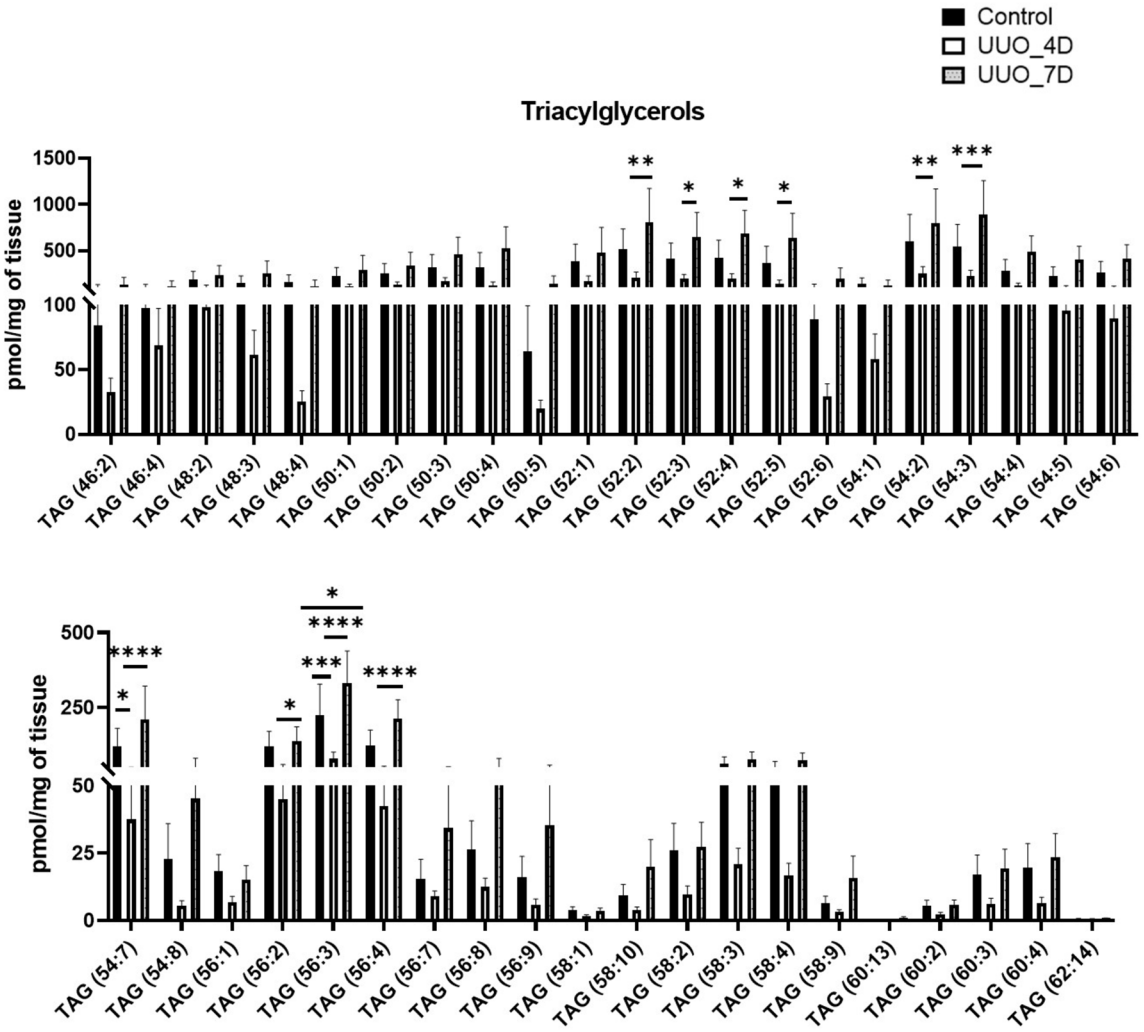

Figure 6. Glycerolipids (triacylglycerols) profile of UUO model after 4 and 7 days compared to control. One-way ANOVA Tukey's multiple comparison tests were applied. A value of $p < 0.05$ (95% confidence level) is considered statistically significant, $^{*}p < 0.05$, $^{**}p < 0.01$, $^{***}p < 0.001$, and $^{****}p < 0.0001$.

strictly on the PIs[42]. Therefore, alteration of the PI system in the kidney results in pathological conditions[42]. Chen et al. report that signaling associated with phosphatidylinositol 3-kinase regulates kidney size in a context-dependent manner to maintain a relatively constant kidney mass/lean body mass ratio[43]. PS is involved in blood coagulation activities and plays a significant role in diabetes and nephrotic syndrome[44,45]. However, with most of the species, a slight alteration with a decreasing trend was observed in the levels of PI and PS levels in the UUO group at day 7 compared to the control (Fig. 4). This alteration may indicate pathological conditions[42], altered kidney mass/lean body mass ratio[43], or apoptotic activities[46].

PC is the major glycerophospholipid in eukaryotic cells[47]. In diabetes, an alteration in PC biosynthesis may contribute to the development of renal hypertrophy[48]. Extensive research suggests that PC plays a pivotal role in many important areas including attenuating acute renal failure and liver dysfunction[49]. Soybean polyunsaturated PC is thought to exert anti-inflammatory activities and has potent effects in attenuating acute renal failure and liver dysfunction[50]. There is no direct evidence of the effects of PC on kidney functions, whereas, as some studies indicate their impacts can cause renal injury. Our analysis results demonstrate the significance of PC lipids in kidney injury as many PCs are significantly reduced in the kidney with UUO (Fig. 5). PEs are one of the most abundant glycerophospholipids in the eukaryotes[51]. Previous studies have indicated their associations with the development of chronic kidney disease (CKD)[52]. Serum PE binding protein 4 (PEBP4) regulates renal functions[53,54], thereby its levels were found significantly elevated and positively correlated with common diagnostic markers in CKD patients[54]. Previous studies indicated CKD events in case of elevated PE, whereas this study found their reduced levels in the UUO model compared with the control group (Fig. 5). These results may indicate some significant correlations with UUO and as plausible targets of kidney injury.

PG is also an important membrane constituent and a key intermediate in the biosynthesis of several lipids including cardiolipins[55]. Previous studies have shown that decreased renal cardiolipin levels can hinder kidney function through mitochondrial dysfunction[56,57]. Cardiolipin therapeutic protects endothelial mitochondria during renal ischemia[58], other studies including this present cardiolipin or its antibodies as an attractive therapeutic,

and diagnostic target in renal transplantation (RT) and kidney diseases[59]. In our studies, PGs and CL showed mixed variations with PG (22:6/22:6) being increased and PG (16:0/18:1), and CL (72:8) decreasing at day 7 of UUO (Fig. 5) indicating their molecular species-specific roles in UUO. Triacylglycerols (TAGs) help the body to produce and regulate hormones, storage, and transport of fatty acids within cells and in the plasma. Increased levels of TAGs characterize Dyslipidemia in CKD[18]. TAG-rich lipoproteins are also found elevated in patients with cardiovascular events in patients with CKD and diabetes[60]. Moreover, adipose triglyceride lipase was found to protect against renal cell endocytosis of CKD in a Drosophila dietary model[61]. Excessive FAs after glyceride esterification may deposit in intracellular lipid droplets in the form of triacylglycerols, which might induce renal damage[35]. As their decreased levels in the previous studies indicate the relevance of cardiovascular or diabetic states, their increment on day 7 of UUO may indicate dyslipidemia in the UUO model (Fig. 6). In fact, in our results the increase of genes associated with lipid droplet formation including Plin 2, and Plin 3 was observed in UUO kidney at day 7 compared to control. The increase of Plin 2 in UUO kidney and Plin 2 as a marker of TAG accumulation was already reported by Mukhi et al.[62] and our results were consistent with this study.

UUO release has been suggested as a viable strategy to reduce kidney injury by improving the glomerular filtration rate and decreasing the inflammatory markers. However, to our knowledge, the effect of UUO release on lipid metabolism has not been investigated. It is interesting to explore whether the lipid changes that occurred during UUO obstruction were reversed or not when the release experiments were conducted. This study has some limitations, including the semi-quantitative lipidomics data and additional experiments are essential to show the fibrosis in the kidney along with mechanisms behind the altered lipids in the UUO model. The number of animals used in these experimental studies is rather small, to make a firm conclusion additional experiments using large animal numbers are necessary. Further studies need to be investigated when UUO is beyond 7 days, UUO kidney vs contralateral kidney comparison in the same mouse, and their effects on lipid metabolism. The study lacks oil-red O staining results to demonstrate the lipid accumulation in the UUO model. Further, this study has another limitation, not all the lipid alterations can be verified at the mRNA level, maybe due to variation between two sets of animals (one set was used for lipid measurement and a second set of mice was used for mRNA validation experiments).

Overall, this study profiles multiple classes of lipid metabolites at molecular species levels and their changes associated with the progression of UUO using a mouse model. The lipid markers discussed in this study are the potential targets for renal injury.

Conclusion

Due to abundance in biological systems and important roles in cell structure and function, lipids were supposed to be crucially associated with kidney disease severity. This study acquired the changes in lipid levels during the progression of kidney injury using the mice UUO model. The established UUO model was confirmed by histochemical analysis and imaging by transmission electron microscopy. The analysis of kidney lipid metabolites from control, 4 and 7 days of UUO groups suggested potentially altered lipid pathways. Compared to the control, a drastic decrease of ceramides, sphingomyelins, and PEs in the UUO group at day 7 appears to be the most promising targets for kidney injury. Further upregulation of ApoE and Plin 2 /Plin 3 genes in UUO kidney at day 7 suggests them as promising markers of acute kidney injury. The studies aiming to understand the mechanism behind these lipid changes are of future interest.

Data availability

All data generated or analyzed during this study are included in the following data depositary "Gowda, Divyavani (2024), "Lipidomic study of kidney in a mouse model with urine flow obstruction", Mendeley Data, V1, Doi: https://doi.org/10.17632/xzrxmmsxwg.1".

Received: 9 August 2023; Accepted: 22 July 2024
Published online: 05 August 2024

References

1. Ntambi, J. M. *Lipid Signaling and Metabolism* (Academic Press, 2020).
2. Zhao, Y.-Y., Vaziri, N. D. & Lin, R.-C. Lipidomics: new insight into kidney disease. *Adv. Clin. Chem.* **68**, 153–175 (2015).
3. Afshinnia, F. *et al.* Lipidomics and biomarker discovery in kidney disease. In *Seminars in Nephrology* 127–141 (Elsevier, 2018).
4. Quehenberger, O. & Dennis, E. A. The human plasma lipidome. *N. Engl. J. Med.* **365**, 1812–1823 (2011).
5. Afshinnia, F. *et al.* Lipidomic signature of progression of chronic kidney disease in the chronic renal insufficiency cohort. *Kidney Int. Rep.* **1**, 256–268 (2016).
6. Chen, H. *et al.* Combined clinical phenotype and lipidomic analysis reveals the impact of chronic kidney disease on lipid metabolism. *J. Proteome Res.* **16**, 1566–1578 (2017).
7. Xu, W. Astragaloside IV ameliorates renal fibrosis via the inhibition of mitogen-activated protein kinases and antiapoptosis in vivo and in vitro. *J. Pharmacol. Exp. Ther.* **350**(3), 552–62. https://doi.org/10.1124/jpet.114.214205. Epub 2014 Jun 20. PMID:24951279. (2014).
8. Chevalier, R. L., Thornhill, B. A., Forbes, M. S. & Kiley, S. C. Mechanisms of renal injury and progression of renal disease in congenital obstructive nephropathy. *Pediatr. Nephrol.* **25**, 687–697 (2010).
9. Klahr, S. & Morrissey, J. Comparative effects of ACE inhibition and angiotensin II receptor blockade in the prevention of renal damage. *Kidney Int.* **62**, S23–S26. https://doi.org/10.1046/j.1523-1755.62.s82.5.x (2002).
10. Warady, B. A. & Chadha, V. Chronic kidney disease in children: The global perspective. *Pediatr. Nephrol.* **22**, 1999–2009 (2007).
11. Martínez-Klimova, E., Aparicio-Trejo, O. E., Tapia, E. & Pedraza-Chaverri, J. Unilateral ureteral obstruction as a model to investigate fibrosis-attenuating treatments. *Biomolecules* **9**, 141 (2019).
12. Manucha, W. Biochemical-molecular markers in unilateral ureteral obstruction. *Biocell* **31**, 1–12 (2007).
13. Aranda-Rivera, A. K., Cruz-Gregorio, A., Aparicio-Trejo, O. E., Ortega-Lozano, A. J. & Pedraza-Chaverri, J. Redox signaling pathways in unilateral ureteral obstruction (UUO)-induced renal fibrosis. *Free Rad. Biol. Med.* **172**, 65–81 (2021).

14. Ucero, A. C. *et al.* Unilateral ureteral obstruction: Beyond obstruction. *Int. Urol. Nephrol.* **46**, 765–776 (2014).
15. Xia, Z.-E., Xi, J.-L. & Shi, L. 3, 3′-Diindolylmethane ameliorates renal fibrosis through the inhibition of renal fibroblast activation in vivo and in vitro. *Renal Fail.* **40**, 447–454 (2018).
16. Banerjee, S. *et al.* Early detection of unilateral ureteral obstruction by desorption electrospray ionization mass spectrometry. *Sci. Rep.* **9**, 1–10 (2019).
17. Agrawal, S., Zaritsky, J. J., Fornoni, A. & Smoyer, W. E. Dyslipidaemia in nephrotic syndrome: Mechanisms and treatment. *Nat. Rev. Nephrol.* **14**, 57–70 (2018).
18. Bulbul, M. C. *et al.* Disorders of lipid metabolism in chronic kidney disease. *Blood Purif.* **46**, 144–152 (2018).
19. Rovin, B. H., Harris, K. P., Morrison, A., Klahr, S. & Schreiner, G. F. Renal cortical release of a specific macrophage chemoattractant in response to ureteral obstruction. *Laboratory Invest. A J. Tech. Methods Pathol.* **63**, 213–220 (1990).
20. Masum, M. A., Ichii, O., Elewa, Y. H. A. & Kon, Y. Podocyte injury through interaction between tlr8 and its endogenous ligand miR-21 in obstructed and its collateral kidney. *Front. Immunol.* **11**, 606488 (2021).
21. Masum, M. A., Ichii, O., Elewa, Y. H. A., Nakamura, T. & Kon, Y. Local CD34-positive capillaries decrease in mouse models of kidney disease associating with the severity of glomerular and tubulointerstitial lesions. *BMC Nephrol.* **18**, 1–12 (2017).
22. Gowda, S. G. B., Sasaki, Y., Hasegawa, E., Chiba, H. & Hui, S. P. Lipid fingerprinting of yellow mealworm Tenebrio molitor by untargeted liquid chromatography-mass spectrometry. *J. Insects Food Feed* **8**, 157–168 (2022).
23. Gowda, S. G. B. *et al.* Docosahexaenoic acid esters of hydroxy fatty acid is a novel activator of NRF2. *Int. J. Mol. Sci.* **22**, 7598 (2021).
24. Mallela, S. K., Merscher, S. & Fornoni, A. Implications of sphingolipid metabolites in kidney diseases. *Int. J. Mol. Sci.* **23**, 4244 (2022).
25. Boini, K. M. *et al.* Acid sphingomyelinase gene deficiency ameliorates the hyperhomocysteinemia-induced glomerular injury in mice. *Am. J. Pathol.* **179**, 2210–2219 (2011).
26. Shiffman, D. *et al.* A gene variant in CERS2 is associated with rate of increase in albuminuria in patients with diabetes from ONTARGET and TRANSCEND. *PLoS ONE* **9**, e106631 (2014).
27. Summers, S. A., Garza, L. A., Zhou, H. & Birnbaum, M. J. Regulation of insulin-stimulated glucose transporter GLUT4 translocation and Akt kinase activity by ceramide. *Mol. Cell. Biol.* **18**, 5457–5464 (1998).
28. Woo, C.-Y. *et al.* Inhibition of ceramide accumulation in podocytes by myriocin prevents diabetic nephropathy. *Diabetes Metab. J.* **44**, 581–591 (2020).
29. Chen, L. *et al.* Unilateral ureteral obstruction causes gut microbial dysbiosis and metabolome disorders contributing to tubulointerstitial fibrosis. *Exp. Mol. Med.* **51**, 1–18 (2019).
30. Malik, R. K., Thornhill, B. A., Chang, A. Y., Kiley, S. C. & Chevalier, R. L. Renal apoptosis parallels ceramide content after prolonged ureteral obstruction in the neonatal rat. *Am. J. Physiol.-Renal Physiol.* **281**(1), F56–F61. https://doi.org/10.1152/ajprenal.2001.281.1.F56 (2001).
31. Morrissey, J., Windus, D., Schwab, S., Tannenbaum, J. & Klahr, S. Ureteral occlusion decreases phospholipid and cholesterol of renal tubular membranes. *Am. J. Physiol.-Renal Physiol.* **250**, F136–F143 (1986).
32. Eckes, T. *et al.* Consistent alteration of chain length-specific ceramides in human and mouse fibrotic kidneys. *Biochim. Biophys. Acta (BBA) Mol. Cell Biol. Lipids* **1866**(1), 158821. https://doi.org/10.1016/j.bbalip.2020.158821 (2021).
33. Ridgway, N. D., Lagace, T. A., Cook, H. W. & Byers, D. M. Differential effects of sphingomyelin hydrolysis and cholesterol transport on oxysterol-binding protein phosphorylation and Golgi localization. *J. Biol. Chem.* **273**, 31621–31628 (1998).
34. Slotte, J. P. & Bierman, E. L. Depletion of plasma-membrane sphingomyelin rapidly alters the distribution of cholesterol between plasma membranes and intracellular cholesterol pools in cultured fibroblasts. *Biochem. J.* **250**, 653–658 (1988).
35. Liu, Z.-X. *et al.* Evaluation of serum free fatty acids in chronic renal failure: Evidence from a rare case with undetectable serum free fatty acids and population data. *Lipids Health Dis.* **18**, 1–9 (2019).
36. Sieber, J. & Jehle, A. W. Free fatty acids and their metabolism affect function and survival of podocytes. *Front. Endocrinol.* **5**, 186 (2014).
37. Wahl, P., Ducasa, G. M. & Fornoni, A. Systemic and renal lipids in kidney disease development and progression. *Am. J. Physiol.-Renal Physiol.* **310**, F433–F445 (2016).
38. Kamijo-Ikemori, A. *et al.* Liver-type fatty acid-binding protein attenuates renal injury induced by unilateral ureteral obstruction. *Am. J. Pathol.* **169**, 1107–1117 (2006).
39. Dai, Y. *et al.* Inhibition of ACSL4 ameliorates tubular ferroptotic cell death and protects against fibrotic kidney disease. *Commun. Biol.* **6**, 907 (2023).
40. Michalczyk, A., Dołęgowska, B., Heryć, R., Chlubek, D. & Safranow, K. Associations between plasma lysophospholipids concentrations, chronic kidney disease and the type of renal replacement therapy. *Lipids Health Dis.* **18**, 1–9 (2019).
41. Tsutsumi, T., Adachi, M., Nikawadori, M., Morishige, J. & Tokumura, A. Presence of bioactive lysophosphatidic acid in renal effluent of rats with unilateral ureteral obstruction. *Life Sci.* **89**, 195–203 (2011).
42. Staiano, L. & De Matteis, M. A. Phosphoinositides in the kidney. *J. Lipid Res.* **60**, 287–298 (2019).
43. Chen, J.-K. *et al.* Phosphatidylinositol 3-kinase signaling determines kidney size. *J. Clin. Invest.* **125**, 2429–2444 (2015).
44. Nagata, S., Suzuki, J., Segawa, K. & Fujii, T. Exposure of phosphatidylserine on the cell surface. *Cell Death Differ.* **23**, 952–961 (2016).
45. Yu, M. *et al.* Phosphatidylserine on microparticles and associated cells contributes to the hypercoagulable state in diabetic kidney disease. *Nephrol. Dial. Transpl.* **33**, 2115–2127 (2018).
46. Leventis, P. A. & Grinstein, S. The distribution and function of phosphatidylserine in cellular membranes. *Annu. Rev. Biophys.* **39**, 407–427 (2010).
47. Payne, F. *et al.* Mutations disrupting the Kennedy phosphatidylcholine pathway in humans with congenital lipodystrophy and fatty liver disease. *Proc. Natl. Acad. Sci. U. S. A.* **111**, 8901–8906 (2014).
48. Suzuki, Y., Fausto, A., Hruska, K. A. & Avioli, L. V. Stimulation of phosphatidylcholine biosynthesis in diabetic hypertrophic kidneys. *Endocrinology* **120**, 595–601 (1987).
49. Rey, J. W. *et al.* Acute Renal failure and liver dysfunction after subcutaneous injection of 3-sn-phosphatidylcholine (Lipostabil®)–case report. *Z. Gastroenterol.* **49**, 340–343 (2011).
50. Jung, Y. Y. *et al.* Protective effect of phosphatidylcholine on lipopolysaccharide-induced acute inflammation in multiple organ injury. *Korean J. Physiol. Pharmacol.* **17**, 209 (2013).
51. Calzada, E., Onguka, O. & Claypool, S. M. Phosphatidylethanolamine metabolism in health and disease. *Int. Rev. Cell Mol. Biol.* **321**, 29–88 (2016).
52. Yang, X. *et al.* Precision toxicology shows that troxerutin alleviates ochratoxin A–induced renal lipotoxicity. *FASEB J.* **33**, 2212–2227 (2019).
53. Afshinnia, F. *et al.* Circulating free fatty acid and phospholipid signature predicts early rapid kidney function decline in patients with type 1 diabetes. *Diabetes Care* **44**, 2098–2106 (2021).
54. He, Q. *et al.* S1P signaling pathways in pathogenesis of type 2 diabetes. *J. Diabetes Res.* **2021**, 1341750 (2021).
55. Stillwell, W. Membrane biogenesis. In *An Introduction to Biological Membranes* 315–329 (Elsevier, 2016). https://doi.org/10.1016/B978-0-444-63772-7.00014-2.
56. Liu, X., Du, H., Sun, Y. & Shao, L. Role of abnormal energy metabolism in the progression of chronic kidney disease and drug intervention. *Renal Fail.* **44**, 790–805 (2022).

57. Yeung, M. H. Y. *et al.* Lipidomic analysis reveals the protection mechanism of GLP-1 analogue dulaglutide on high-fat diet-induced chronic kidney disease in mice. *Front. Pharmacol.* https://doi.org/10.3389/fphar.2021.777395 (2022).
58. Liu, S., Soong, Y., Seshan, S. V. & Szeto, H. H. Novel cardiolipin therapeutic protects endothelial mitochondria during renal ischemia and mitigates microvascular rarefaction, inflammation, and fibrosis. *Am. J. Physiol.-Renal Physiol.* **306**, F970–F980 (2014).
59. Miranda-Díaz, A. G., Cardona-Muñoz, E. G. & Pacheco-Moisés, F. P. The role of cardiolipin and mitochondrial damage in kidney transplant. *Oxidat. Med. Cell. Longev.* **2019**, 1–13 (2019).
60. Sidney, S. *et al.* Recent trends in cardiovascular mortality in the United States and public health goals. *JAMA Cardiol.* **1**, 594–599 (2016).
61. Lubojemska, A. *et al.* Adipose triglyceride lipase protects renal cell endocytosis in a Drosophila dietary model of chronic kidney disease. *PLoS Biol.* **19**, e3001230 (2021).
62. Mukhi, D. *et al.* ACSS2 gene variants determine kidney disease risk by controlling de novo lipogenesis in kidney tubules. *J. Clin. Invest.* https://doi.org/10.1172/JCI172963 (2023).

Acknowledgements

This work is supported by the Japanese Society for the Promotion of Science KAKENHI Grants (19H0311719, 19F19092, 19K0786109, 22K1485002, and 21K1481201).

Author contributions

S.G., M.A.M., O.I., Y.K., and S.G.B. carried out the experiments; S.G.B., H.C., and S-P.H. supervised the study and contributed toward the discussion; M.A.M., C.S., and D.G., wrote the first draft. All authors have read and approved the final manuscript.

Competing interests

The authors declare no competing interests.

Additional information

Supplementary Information The online version contains supplementary material available at https://doi.org/10.1038/s41598-024-68270-5.

Correspondence and requests for materials should be addressed to M.A.M. or S.-P.H.

Reprints and permissions information is available at www.nature.com/reprints.

Publisher's note Springer Nature remains neutral with regard to jurisdictional claims in published maps and institutional affiliations.